Tunneling

DOI: 10.1002/anie.201001311

Hydrogen-Atom Tunneling Could Contribute to H_2 Formation in Space**

Theodorus P. M. Goumans and Johannes Kästner*

The interaction of hydrogen atoms with graphite and aromatic hydrocarbons is widely studied because it plays an important role in diverse areas, such as plasma-wall interactions in nuclear fusion reactors,[1,2] hydrogen-storage materials,[3] petroleum refining,[4] and H_2 formation in space.[5–10] H addition to benzene is the rate-determining step in the surface-catalyzed conversion of benzene into cyclohexane.[11] H atoms can also chemisorb on graphite,[9] although the carbon atom to which it binds has to pucker out of the plane, resulting in an activation barrier of about 20 kJ mol^{-1}.[12,13] Chemisorption on the edge of a polycyclic aromatic hydrocarbon (PAH) is predicted to have a much lower activation barrier[14] and, more strikingly, for some configurations there is no activation barrier for the reaction with a second H atom, yielding either chemisorbed H_2 or gaseous H_2.[7,15]

In industry, the surface hydrogenation of benzene occurs at high temperatures[4] and Arrhenius behavior is observed between 370 and 300 K,[11,16] where tunneling does not (yet) play a role. In the interstellar medium (ISM), however, temperatures are much lower, ranging from 10 K in molecular clouds to 100 K in diffuse clouds and up to several hundred K in photon-dominated regions (PDRs) near young stellar objects. In all these regions H_2 is very abundant despite inefficient gas-phase formation routes and H_2 destruction by cosmic rays and photons. Astrochemical models require facile chemisorption of H on carbonaceous dust grains at intermediate temperatures to account for the observed abundances of interstellar H_2.[17,18] Especially in PDRs, the H_2 formation rate should be relatively high and is predicted to be catalyzed by H chemisorption on small PAHs.[19] Furthermore, the inclusion of tunneling by an approximate model explains the observed deuterium enrichment in molecular hydrogen.[17] Quantitative tunneling rates, however, depend strongly on the barrier height and shape. We performed rate calculations allowing for tunneling in all spatial dimensions for the low-temperature addition of H and D atoms to benzene as a simple model for PAHs.

To evaluate accurate tunneling rates at low temperatures for many-atom systems with asymmetric barriers, we employ harmonic quantum transition-state theory (HQTST),[20,21] also known as instanton[22,23] or ImF[24] theory. The rate is calculated using quantum statistical mechanics by discretized closed Feynman path (CFP) integrals. Analogous to classical harmonic transition-state theory, the quantum transition state (qTS) is a first-order saddle point in the space of CFPs. The vibrational modes of the reactant state and the modes orthogonal to the tunneling path are expanded harmonically.[20,21] This approach has been shown to be quite accurate in comparison to analytic solutions and results from quantum dynamics, especially at low temperatures where other semiclassical tunneling approaches often underestimate transmission coefficients.[21]

To enable HQTST calculations of many-atom systems, we employ direct dynamics by an interface between the recent HQTST code[20,21] and ChemShell.[25] This method allows the optimization of the CFP to a saddle point, the qTS (or instanton), by obtaining forces and energies directly from a quantum mechanics (QM) or molecular mechanics (MM) program, or a QM/MM combination thereof. With decreasing temperature, tunneling is enhanced and the qTS becomes more delocalized. Consequently, more images are needed to resolve the CFP, involving thousands of force evaluations, to obtain HQTST rates at temperatures as low as 10 K. The direct dynamics HQTST approach for many-atom systems therefore requires relatively efficient computational methods, such as DFT or semi-empirical Hamiltonians that reproduce reasonably well the features of the potential energy surface (PES), in particular the height and shape of the classical transition state, because tunneling strongly depends on both of them.[26] We tested common functionals with a 6-31G*(*) basis against high-level CCSD(T)/CBS calculations (Table 1).

The MPWB1K functional[27] gives values in closest agreement with the benchmark ab initio method, while functionals with less or no exact exchange give much lower barriers, as has also been observed previously for other reactions relevant to the ISM.[28,29] The B3LYP, PBE, and PW91 calculated classical transition-state theory (TST) reaction rates are always higher than the experimental rates,[30,31] while the CCSD(T) and MPWB1K reaction rates are lower at low temperatures (Supporting Information). The CCSD(T)/CBS

[*] Dr. T. P. M. Goumans
Gorlaeus Laboratories, LIC, Leiden University
P.O. Box 9502, 2300 RA Leiden (The Netherlands)
Fax: (+31) 71-527-4397
E-mail: t.goumans@chem.leidenuniv.nl
Homepage: http://theor.lic.leidenuniv.nl/people/goumans
Prof. J. Kästner
Computational Biochemistry Group, Universität Stuttgart
Pfaffenwaldring 55, 70569 Stuttgart (Germany)

[**] This work is financially supported by the Netherlands Organisation for Scientific Research (NWO) through a VENI-fellowship (700.58.404) for T.P.M.G., the German Research Foundation (DFG) through the Cluster of Excellence SimTech (EXC 310/1) at Universität Stuttgart for J.K., and the European Commission (project number 228398) through an HPC-Europa2 project. Prof. H. Jónsson, Prof. G.-J. Kroes, and Prof. E. F. van Dishoeck, and Dr. S. Andersson and Dr. A. Arnaldsson are acknowledged for useful discussions.

Supporting information for this article is available on the WWW under http://dx.doi.org/10.1002/anie.201001311.

Table 1: Calculated barriers (including ZPE)[a] for $H + C_6H_6$ [kJ mol^{-1}].

CCSD(T)	MPWB1K	B3LYP	PBE	PW91
22.9	23.7	13.6	12.9	11.6

[a] CCSD(T)/CBS values include zero-point energies (ZPE) at the CCSD level, all DFT values include ZPE at the DFT level.

and MPWB1K/6-31G*(*) vibrationally adiabatic barriers are in good agreement with each other, but are slightly higher than the experimental activation energy of 18.0 kJ mol^{-1},[30] while the other functionals have slightly lower barriers. The MPWB1K geometry of the $H + C_6H_6$ transition state is closest to the CCSD/cc-pVDZ one, while the other functionals predict much earlier (larger C–H distances) transition states. Moreover, the energies of relevant points along the qTS calculated with CCSD(T)-F12[32] are in very good agreement with the MPWB1K results (Supporting Information).Therefore, MPWB1K/6-31G*(*) is our method of choice for the direct dynamics rate calculations for the $H/D + C_6H_6$ reactions.

The cross-over temperature T_c, the temperature below which HQTST can be used and below which tunneling becomes the main mechanism, for H + benzene is 222 K, while that for D + benzene is 171 K, in agreement with the notion that tunneling should be less important for the addition of the heavier deuterium atom. Nevertheless, tunneling will dominate the reaction rates for both H and D addition reactions in the ISM at temperatures between 10 and 100 K. The delocalization along the transition coordinate that results from such strong tunneling behavior is nicely illustrated by the qTS (a 170 image CFP) for $H + C_6H_6$ at 20 K depicted in Figure 1. While clearly the tunneling motion is largely associated with the motion of the incoming hydrogen atom, the heavier carbon atoms also delocalize and contribute to the tunneling rate.

The calculated HQTST reaction rates for H and $D + C_6H_6$ are plotted in an Arrhenius plot in Figure 2, along with the reaction rates from classical TST with quantized harmonic vibrations. The strong deviation of the HQTST rates from the

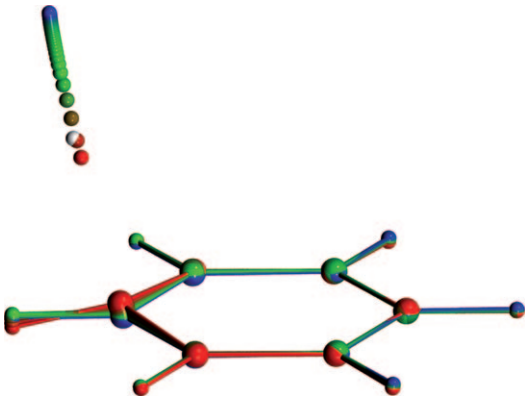

Figure 1. The delocalization in the quantum transition-state (qTS) for H + benzene at 20 K is a clear sign of strong quantum tunneling involving more than one atom. Besides the incoming hydrogen, the benzene skeleton is also delocalized. The white sphere indicates the position of the hydrogen in the classical transition state. The uneven distribution of the images indicates a highly asymmetric barrier with a shallow minimum at the reactant side (blue) and a deep one at the product side (red).

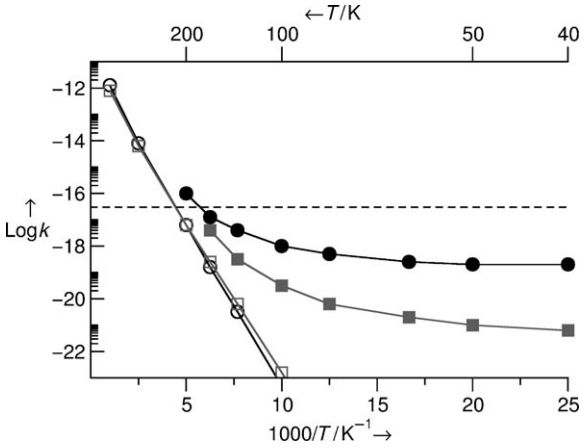

Figure 2. Logarithm of HQTST and classical TST rate constants for H + benzene and D + benzene versus inverse temperature. Black circles: H; gray squares: D; closed symbols: HQTST; open symbols: classical TST. The rate constant k is given in cm^3 molecule^{-1} s^{-1}, dashed black line: $k = 3 \times 10^{-17}$ cm^3 molecule^{-1} s^{-1}.

linear relationship between log k and $1/T$ for the classical TST rates is a clear signature of strong tunneling behavior.

At low temperatures, where only ground-state vibrational levels are occupied, classical TST predicts an inverse kinetic isotope effect (KIE) because in the transition state the zero-point energy is lower for the forming C–D bond than for the C–H bond (Supporting Information). At very high temperatures, where more vibrational levels are occupied, however, H addition is marginally faster than D addition, because the relative translational partition function is larger for the heavier D atom. However, because H tunnels much more efficiently than D, HQTST predicts a very high positive KIE at $T < T_c$.

The long time scales in the ISM (ca. 10^5 year) make the rate for addition to benzene relevant for H at 40 K and D at 120 K ($k \approx 10^{-19}$ cm^3 molecule^{-1} s^{-1}). For the surface-catalyzed hydrogenation of benzene there is an apparent activation energy of 41 kJ mol^{-1},[16] which makes the classical rates at the T_c (222 K) already very low and therefore any tunneling effect at lower temperatures would be very hard to observe experimentally. The tunneling path for the surface reaction will also differ from that in the gas phase.

If H atoms could indeed chemisorb on PAHs, this would be an efficient mechanism for the formation of HD and H_2 in warmer regions of the ISM.[18] The addition of a second H or D atom is barrierless *para* to a chemisorbed H on a graphitic system[7,15] or next to a H chemisorbed on the edge of a PAH.[14] Likewise, direct abstraction by a gas-phase H atom (Eley–Rideal formation of H_2) is (nearly) barrierless for H chemisorbed on graphite[12,33] or on the edge of a PAH.[14] Furthermore it has been suggested that the surplus energy from the strongly exothermic addition of a second hydrogen could also yield H_2 by an indirect, "dimer-mediated" reaction mechanism.[10]

Whatever the precise mechanism of H_2 formation in the ISM by chemisorbed atoms, the chemisorption of the first H atom to a carbonaceous particle is rate-limiting. To reproduce observed H_2 abundances in diffuse clouds and PDRs, it has been suggested that the H_2 formation rate exceeds 3×10^{-17} or

2×10^{-16} cm^3 molecule^{-1} s^{-1}.[19] Our calculations indicate that H-addition to benzene can reach 3×10^{-17} molecule^{-1} s^{-1} at approximately 180 K (Figure 2), while D will chemisorb an order of magnitude slower. Since the functional we used overestimates the classical barrier, the real rates will be higher than our calculated ones. The classical barrier for H addition to PAHs is lower at edge sites and higher at core sites.[14] The lower classical barriers will also lead to much higher HQTST rates for H chemisorption on the edges of a variety of PAHs, which could account for the high H_2 formation rates in diffuse clouds and PDRs suggested by observations. Likewise, the fast H chemisorption and abstraction on amorphous carbon could contribute significantly.[34] The relative importance of these two types of carbon grains as catalysts for H_2 formation will depend on the tunneling rate of the rate-limiting step (addition or abstraction), as well as the relative concentration of active sites, PAHs edge atoms or exposed active C-atoms.

In conclusion, we have presented a direct dynamics implementation of HQTST, which allows the calculation of accurate reaction rates where tunneling is important. Indeed, HQTST calculations for H + benzene suggest that H atoms could chemisorb on PAHs in the moderately warm (100–200 K) regions of the ISM, contributing to the catalytic formation of H_2.

Experimental Section

The DFT calculations of Table 1 were performed with Gaussian 03[35] with the same 6-31G*(*) basis as for the qTS: 6-31G* for benzene and 6-31G** for the incoming H atom. The CCSD(T)/CBS calculations were performed with Molpro.[36] The Hartree–Fock (HF) ($n = 2,3,4$) and correlation energies ($n = 3,4$) are extrapolated[37] with the correlation consistent basis sets cc-pVnZ[38] on the CCSD/cc-pVDZ optimized geometries. CCDS(T)-F12/cc-pVTZ energies are in good agreement with these CCSD(T)/CBS energies. Unscaled ZPEs were added at the level at which the structures were optimized (DFT, CCSD/cc-pVDZ).

The HQTST methodology is described in refs. [20–24] and is briefly reviewed in the Supporting Information. The qTS is a first-order saddle point on the minimum action path in the N × P dimensions spanned by the CFPs, where N = 3 × number of atoms and P = number of images of the CFP. The qTS is optimized using a mode-following algorithm with the minimum mode found by the Lanczos algorithm,[39] and the overall optimization carried out with the limited-memory formulation of the Broyden-Fletcher-Goldfarb-Shanno algorithm (L-BFGS).[40] Forces and energies were used from NWChem,[41] with the MPWB1K functional on a fine integration grid. To calculate the harmonic modes of the qTS we used Gaussian 03[35] to calculate the analytical hessian of each point of the CFP, using an ultrafine grid. NWChem and G03 energies were in agreement to within 15 μH.

Received: March 4, 2010
Revised: May 21, 2010
Published online: August 2, 2010

Keywords: ab initio calculations · astrochemistry · hydrogen · kinetics · tunneling

[1] S. Morisset, A. Allouche, *J. Chem. Phys.* **2008**, *129*, 024509.
[2] W. Jacob, C. Hopf, M. Schlüter, *Phys. Scr. T* **2006**, *124*, 32–36.
[3] W. C. Xu, K. Takahashi, Y. Matsuo, Y. Hattori, M. Kumagai, S. Ishiyama, K. Kaneko, S. Iijima, *Int. J. Hydrogen Energy* **2007**, *32*, 2504–2512.
[4] B. H. Cooper, B. B. L. Donnis, *Appl. Catal. A* **1996**, *137*, 203–223.
[5] J. Kerwin, B. Jackson, *J. Chem. Phys.* **2008**, *128*, 084702.
[6] R. Papoular, *Mon. Not. R. Astron. Soc.* **2005**, *359*, 683–687.
[7] L. Hornekaer, E. Rauls, W. Xu, Z. Sljivancanin, R. Otero, I. Stensgaard, E. Laegsgaard, B. Hammer, F. Besenbacher, *Phys. Rev. Lett.* **2006**, *97*, 186102.
[8] S. Casolo, O. M. Lovvik, R. Martinazzo, G. F. Tantardini, *J. Chem. Phys.* **2009**, *130*, 054704.
[9] T. Zecho, A. Guttler, X. W. Sha, B. Jackson, J. Kuppers, *J. Chem. Phys.* **2002**, *117*, 8486–8492.
[10] H. M. Cuppen, L. Hornekaer, *J. Chem. Phys.* **2008**, *128*, 174707.
[11] K. M. Bratlie, C. J. Kliewer, G. A. Somorjai, *J. Phys. Chem. B* **2006**, *110*, 17925–17930.
[12] X. W. Sha, B. Jackson, *Surf. Sci.* **2002**, *496*, 318–330.
[13] L. Jeloaica, V. Sidis, *Chem. Phys. Lett.* **1999**, *300*, 157–162.
[14] E. Rauls, L. Hornekaer, *Astrophys. J.* **2008**, *679*, 531–536.
[15] N. Rougeau, D. Teillet-Billy, V. Sidis, *Chem. Phys. Lett.* **2006**, *431*, 135–138.
[16] K. M. Bratlie, G. A. Somorjai, *J. Phys. Chem. C* **2007**, *111*, 6837–6845.
[17] S. Cazaux, P. Caselli, V. Cobut, J. Le Bourlot, *Astron. Astrophys.* **2008**, *483*, 495–508.
[18] S. Cazaux, A. G. G. M. Tielens, *Astrophys. J.* **2004**, *604*, 222–237.
[19] E. Habart, F. Boulanger, L. Verstraete, C. M. Walmsley, G. P. des Forets, *Astron. Astrophys.* **2004**, *414*, 531–544.
[20] S. Andersson, G. Nyman, A. Arnaldsson, U. Manthe, H. Jónsson, *J. Phys. Chem. A* **2009**, *113*, 4468–4478.
[21] A. Arnaldsson, PhD thesis, University of Washington, **2007**.
[22] C. G. Callan, S. Coleman, *Phys. Rev. D* **1977**, *16*, 1762–1768.
[23] W. H. Miller, *J. Chem. Phys.* **1975**, *62*, 1899–1906.
[24] I. Affleck, *Phys. Rev. Lett.* **1981**, *46*, 388–391.
[25] P. Sherwood et al., *J. Mol. Struct.* **2003**, *632*, 1–28. (For authors, see the Supporting Information.)
[26] L. B. Harding, S. J. Klippenstein, A. W. Jasper, *Phys. Chem. Chem. Phys.* **2007**, *9*, 4055–4070.
[27] Y. Zhao, D. G. Truhlar, *J. Phys. Chem. A* **2004**, *108*, 6908–6918.
[28] T. P. M. Goumans, W. A. Brown, C. R. A. Catlow, *J. Phys. Chem. C* **2008**, *112*, 15419–15422.
[29] T. P. M. Goumans, M. A. Uppal, W. A. Brown, *Mon. Not. R. Astron. Soc.* **2008**, *384*, 1158–1164.
[30] J. M. Nicovich, A. R. Ravishankara, *J. Phys. Chem.* **1984**, *88*, 2534–2541.
[31] Y. Gao, N. J. DeYonker, E. C. Garrett, A. K. Wilson, T. R. Cundari, P. Marshall, *J. Phys. Chem. A* **2009**, *113*, 6955–6963.
[32] T. B. Adler, H.-J. Werner, *J. Chem. Phys.* **2009**, *130*, 241101–241105.
[33] R. Martinazzo, G. F. Tantardini, *J. Chem. Phys.* **2006**, *124*, 124702.
[34] V. Mennella, *Astrophys. Lett. Commun.* **2008**, *684*, L25–L28.
[35] Gaussian 03 (Revision D.01), M. J. Frisch et al., **2003**. (For authors, see the Supporting Information.)
[36] MOLPRO (version 2008.1), H. J. Werner et al. (For authors, see the Supporting Information.)
[37] T. Helgaker, W. Klopper, H. Koch, J. Noga, *J. Chem. Phys.* **1997**, *106*, 9639–9646.
[38] T. H. Dunning, Jr., *J. Chem. Phys.* **1989**, *90*, 1007–1023.
[39] R. A. Olsen, G. J. Kroes, G. Henkelman, A. Arnaldsson, H. Jónsson, *J. Chem. Phys.* **2004**, *121*, 9776–9792.
[40] D. C. Liu, J. Nocedal, *Math. Program.* **1989**, *45*, 503–528.
[41] NWChem (Version 5.1.1), T. P. Straatsma et al.. (For authors, see the Supporting Information.)

